The Effect of Globular Protein from Aleurone Cells of Barley on Stearic Acid Monolayers

ILEANA COJOCARU[1], ANDRADA TOMOAIA COTISEL[2], AURORA MOCANU[3], TRAIANOS YUPSANIS[4], MARIA TOMOAIA COTISEL[3,5]*

[1]University of Craiova, 13 A.I. Cuza Str., 200585, Craiova, Romania

[2]London School of Hygiene and Tropical Medicine, Keppel Street, London WC1E 7HT, UK,

[3]Babes-Bolyai University of Cluj-Napoca, Faculty of Chemistry and Chemical Engineering, Chemical Engineering Department, 11 Arany Janos Str.,400028 Cluj Napoca, Romania

[4]Aristotelian University, School of Chemistry, Laboratory of Biochemistry, 54006 Thessaloniki, Greece

[5]Academy of Romanian Scientists, 54 Splaiul Independentei, 050094, Bucharest, Romania

Aleurone cells of barley accumulate the major storage globular protein, which is deposited in different patterns, such as protein and lipid self-assemblies. To better understand the complexity of storage self-assemblies, a fatty acid is chosen as a lipid model, namely stearic acid, SA, because of its high stability in monolayers at the air/aqueous solutions interface. The effect of aleurone cell protein, AC protein, on the phase behavior and surface structure of SA monolayers at the air/water interface has been studied by a combined Langmuir and Langmuir-Blodgett (LB) technique and by atomic force microscopy (AFM) investigation. The AC protein and SA monolayers were transferred on glass support, at several controlled surface pressures, characteristic for both the condensed liquid and solid phase of pure SA monolayers. The results indicate that globular particles of AC protein adsorb on and penetrate into and specifically interact with SA monolayers stabilizing the lipid/protein interface by achieving highly ordered self-assemblies, which may also occur within aleurone layers. These structures might play an important role both in aleurone cell development and in seedling growth.

Keywords: Aleurone cell major storage protein, globular protein, stearic acid, AFM, LB technique

It has already been demonstrated that cereal seeds accumulate globular storage proteins [1-11] and oils, such as fatty acids and lipids [6], assembled usually as granules within aleurone cells. Understanding of their self-assemblies formation may contribute to further design and engineer new biomaterials, at nanoscale level, essential for biological, medical and nutritional applications.

Mostly, storage proteins are deposited in different patterns in aleurone layers, due to various factors that mediate the protein body formation [3, 9]. Among these, the protein interactions with various storage lipids may determine the protein and lipid assemblies within the aleurone layers. Consequently, the structural characterization of these biomolecules in self assemblies is of a great interest, especially in the relation with the protein-lipid body formation and with the mobilization of these reserve materials during germination.

The major storage globular protein was identified and extracted from aleurone cells of barley, and was well purified as presented elsewhere [1]. This globular protein is comprised of four independent subunits with relative molecular masses of 50, 40, 25 and 20 kDa [1]. It belongs to globulins, which are soluble in dilute salt aqueous solutions.

This aleurone cell protein, AC protein, was previous investigated by us, regarding its secondary structure [12-14]. The results indicate a dominant α-helix structure for AC protein and a rather high thermal stability up to 60 °C, making this protein important for biological and pharmacological uses. However, some contributions from β-sheet, turns and random coil structures are not excluded.

We also explored the AC protein self-assemblies in coating layers on solid surfaces [15, 16] and its nanostructure formation in bulk [17, 18] and at interfaces [19, 20]. The globular AC protein was used by us in premiere to functionalize gold nanoparticles, GNPs [18, 19]. The resulting supramolecular assemblies may contribute to the development of innovative drug delivery systems [21, 22].

Generally, the adsorption kinetics of biomolecules at oil/water [20, 23-25] and air/water interfaces [20, 26] is a crucial step for the evaluation of their surface active properties. In this context, the AC protein [20] and various plant proteins [23] showed a high stability in oriented interfacial layers. Further, a thermodynamic approach of phase equilibria of biomolecules spread at the air/water interface [27-36] brings knowledge on the behavior of membrane models, such as monolayers at fluid interfaces.

Aleurone cells also store and metabolize large quantities of oils, fatty acids and lipids, which occupy up to 30% of their cellular volumes [6]. The presence of rather big amount of lipids in aleurone cells rationally leads to the question related to their interactions with storage proteins. However, this aspect has not yet been thoroughly investigated in the state of the art.

The general opinion on the biological cells is related to the interaction of lipids and proteins to accomplish membrane organization and function [37-43] as well as to achieve the physical and chemical processes in biological systems. Certainly, the lipid layer can induce protein-protein interaction and influence cellular signaling and trafficking. Understanding these processes will provide valuable data about the mechanism by which plant cells achieve higher order tissue organization.

The lipid-protein interactions can be examined by using monolayer techniques [39, 40, 61, 62], which offer controlled conditions for the formation of self-assemblies. Additionally, the packing of biomolecules at interfaces can also be measured [33-36]. Furthermore, Langmuir-Blodgett (LB) technique offers the possibility for the transfer of monolayers from air/water interface to solid support at a

* *email: mcotisel@gmail.com*

chosen constant surface pressure [44-48] for further structural investigation, using for example, the atomic force microscope (AFM).

AFM allows the localization of associated proteins to lipid monolayers, without the need for fluorescence staining. AFM also offers the possibility for the determination of surface roughness on model membranes [49-51] and on natural membranes [52]. Hence, AFM is a technique of choice to study highly ordered layers of different materials [53-56].

This work presents the cutting-edge investigation on the self-assemblies of globular AC protein with lipids at fluid interfaces by combined Langmuir and Langmuir-Blodgett (LB) technique coupled with atomic force microscopy (AFM). As lipid model, stearic acid is used, because of several reasons, such as its high stability in membrane models, high capability of sensing variations in pH and ionic strength of aqueous media, and possess well-characterized phase behavior in oriented layers [28, 48].

The association of lipids and AC protein in aleurone cells might take part in the regulation process of the steady state existing in dormancy period as well as in the early steps of reserve material mobilization during the germination phase.

Experimental Part

Materials and methods

The aleurone cell protein, AC protein, of barley was extracted and purified as previously described [1]. The AC protein is a mixture of four closely related peptides of about 20, 25, 40 and 50 kDa. These subunits are not associated by interchain disulphide bonds. Furthermore, it was evidenced a high stability of the globular shape of protein molecules, through strong hydrophobic interactions among hydrophobic parts of these peptides.

The AC protein powder, about 5 mg L^{-1}, was dissolved in aqueous solution, containing 0.5 M NaCl, of *p*H 5.3, using ultrapure water of 18 Mohm cm, at 25°C, obtained in Elgastat system.

The stearic acid (SA) and NaCl were purchased from Sigma. The n-hexane, used for the spreading of SA molecules at the air/aqueous solution interface, was purchased from Merck.

Langmuir monolayer technique

The stearic acid monolayers were obtained by spreading a known number of SA molecules in organic solution (e.g. n-hexane) on the air/aqueous solution interface [28, 48] of a precise known area in a teflon trough. Our automatic Langmuir equipment is KSV 5000, manufactured in Finland. The area of the SA (Langmuir) monolayer is compressed by teflon barriers placed across the teflon trough. Consequently, the mean molecular area (A, $Å^2$/molecule) of SA is accurately determined. Simultaneously, the surface pressure, π in mN/m, is measured using surface tension sensor with Wilhelmy plate method [48].

Langmuir-Blodgett (LB) technique and LB layers deposition. Langmuir equipment needs additional capabilities of dipping a particular solid support (e.g., glass optically polished and very well cleaned) through the SA Langmuir layer, at a controlled speed, while the SA monolayer is kept at a chosen constant surface pressure, at the air/aqueous solutions interface. Accordingly, the LB layer is engineered by vertically passing the hydrophilic glass from the aqueous phase through the SA monolayer upwards to the air phase, while the SA monolayer is maintained at the chosen surface pressure. Certainly, the resulting LB sample can be a single layer or a multilayer depending on the number of passes made through the SA monolayer. Evidently, one LB layer is transferred on the glass plate during each pass.

Typically, the transfer ratio is determined as the ratio between the decreased area of Langmuir monolayer and the total surface area of the glass support. A transfer ratio of unity indicates that an excellent LB layer is transferred. Under appropriate conditions, the structure of the Langmuir monolayer is preserved during the LB layer transfer from air/aqueous solutions interface to glass plate and a replica of the Langmuir monolayer is obtained on glass support.

Atomic force microscopy (AFM). AFM operated in tapping mode is a high resolution surface imaging technique for the determination of size and shapes of various nanostructures [48, 56] and for the analysis of different self-assemblies [18, 19]. In the current study, AFM is used coupled with LB technique for the visualization of supramolecular assemblies [45-48] and for surface roughness evaluation [12, 52]. All AFM measurements were performed on LB layers of SA spread on aqueous solution of 0.5 M NaCl, in the absence and the presence of AC protein (e.g., 5 mg/L).

Results and discussions

To assure that the adsorption equilibrium of AC protein onto SA monolayer is reached within a practical time (e.g., about 30 min), a rather high concentration of AC protein, about 5 mg/L, was chosen in aqueous solutions of 0.5 M NaCl, at *p*H 5.3, as estimated from AC protein adsorption kinetics [20] at fluid interfaces. Accordingly, each compression isotherms at air/aqueous solution interface was performed in about 60 min.

It is to be noted that, this concentration of AC protein in aqueous subphase is the same with the concentration of cytochrome c used in the investigation of its adsorption to phospholipid monolayers, studied by reflection spectroscopy, at the air/solution interface [39].

Firstly, the globular AC protein is dissolved in the aqueous phase of 0.5 M NaCl, at the chosen concentration (e.g., 5 mg L^{-1}) and the resulting *p*H is 5.3. At this *p*H, taking into account the thermodynamics of interfacial protolytic equilibria the stearic acid spread at the air/aqueous solutions interface is about 50% neutral and 50% negatively charged [28, 34-36]. Then, stearic acid monolayer is spread at the air/aqueous phase interface in a Langmuir trough, at a selected spreading area of about 30 $Å^2$/molecule, in the absence of AC protein, and at about 103 $Å^2$/molecule, in the presence of AC protein, at rather low spreading surface pressures (fig. 1). After that, the entire system is kept for 30 minutes at room temperature (22°C) for the evaporation of the organic solvent, which is used for stearic acid spreading, and for reaching an internal equilibrium within the spread SA layer. Subsequently, at least 10 compressional isotherms, in terms of surface pressure, π in mN/m, versus mean molecular area, A in $Å^2$/molecule, are recorded at a compression rate of 0.7 cm/min, and the representative isotherms are given in figure 1.

Secondly, at a chosen constant surface pressure, both the pure SA monolayer and mixed SA/AC protein self-assemblies are transferred from air/aqueous solutions interface to glass surface at a constant transfer rate of about 0.5 cm/min, thus, reaching a transfer ratio of about 1. Lastly, the transferred LB layers on glass are explored with AFM imaging.

These experiments give clear information on the penetration capacity of AC protein into the interfacial SA layer, allowing a direct access to the area of expanded SA layer caused by the AC protein penetration, at a particular constant surface pressure. As an example, at the spreading

area of SA on AC protein aqueous subphase, at about 103 Å²/molecule of SA, the spreading surface pressure is about 1.5 mN/m. The expanded area is given by the difference between spreading SA area, in the presence of protein, and the pure SA area of about 28 Å²/molecule, and corresponds to the same lateral pressure (i.e., 1.5 mN/m). Accordingly, the expanded SA area is about 75 Å²/molecule.

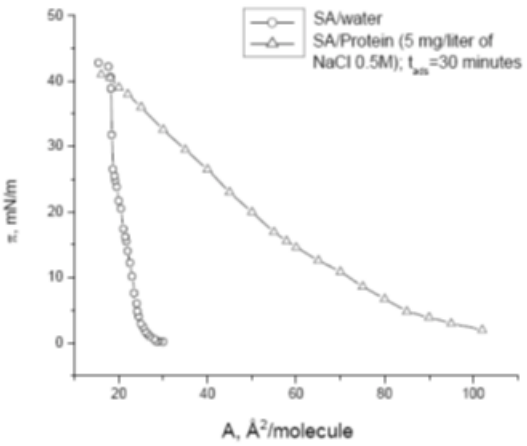

Fig. 1. Compressional isotherms of stearic acid (SA) monolayers spread at the interface: air/aqueous solutions of 0.5 M NaCl, in the absence (O) and the presence of AC protein, at a concentration of 5 mg/L (Ä). The time allowed for the adsorption (t_{ads}) of AC protein to SA spread monolayer is 30 min, before the compression of mixed layer.

During the compression of mixed SA/AC protein interfacial layer, the expanded area per SA molecule is decreased and becomes zero near the collapse of the pure SA layer at about 43 mN/m (fig. 1 and table 1). The collapse pressure is the highest surface pressure reached for a monolayer highly packed without the detection of collapsed bulk phase [34].

In addition, the phase transition from condensed liquid to solid state in pure SA layer, at about 25.5 mN/m (fig. 1), is abolished in the presence of AC protein. Moreover, during compression of mixed interfacial SA/AC protein layer, the AC protein aggregates and at the high surface pressure near the SA collapse (43 mN/m), the AC protein is squeezed out from SA layer (A_c values are identical, tabel 1) and remains attached to SA layer (as visualized in the following AFM images). Consequently, the interaction of AC protein with the SA layer led to a very high stability of the mixed SA/AC protein layer, compactly packed at interface.

Moreover, inspecting the compressional isotherms in Fig. 1, it can be observed that the AC protein displays rather high affinity for SA monolayer, especially for SA liquid phase. This aspect is also supported by the surface characteristics of SA monolayers (table 1), namely the limiting molecular area, A_0, which corresponds to the molecular area of SA molecules, obtained by the extrapolation of linear portion of the compressional isotherms for surface pressure equals zero, and A_c is the collapse area of SA molecules at collapse pressure.

AFM was used for probing the self-assemblies of globular AC protein, obtained by protein adsorption from aqueous solution on the surface of glass (figs. 2a-2c), at nanometric resolution. The governing factors found to affect the AC protein layer stability were *p*H, that controls the net charge on the protein surface and the surface roughness associated with the solid-liquid interface. The AFM images showed the formation of the nanoparticles of AC protein, mainly spherical particles, self-assembled within the stable adsorbed layer on glass. The size of AC protein nanoparticles is of tens of nm in the range of 40 to 70 nm, predominantly of 50 to 55 nm (fig. 2d), but the smallest particles with diameter of 20 nm or larger particles of 80 nm are still evidenced, in substantial agreement with other recent studies on different globular proteins [57-59].

We suggest that AC protein molecules can auto-associate as the AC protein nanoparticles, which occur and self-assemble at an interface either at air/liquid interface or at glass/liquid interface. This surface-mediated aggregation can be driven, by the favorable interaction of hydrophobic patches in the AC protein, which might become exposed during AC protein adsorption [58]. Besides of this, a bulk aggregation of AC protein molecules cannot be completely rule out in aqueous solutions, while precise mechanism remains debatable.

On the other hand, even at iso-electric *p*H, AC protein molecule possesses patches of negative and positive charges on its surface, although its net surface charge is zero. Hence, an aggregation of AC protein molecules can be also promoted by charge-induced dipole interactions.

The upper surface of pure AC protein layers is nearly flat, as it is given by RMS value of 1.18 nm. This aspect is important for the deposition of an additional protein layer, by either strong interactions or high affinity protein and protein interactions. The high stability of globular AC protein adsorbed layers might be of great interest for potential therapeutic uses of this protein.

Monolayer	A_0, Å²	A_c, Å²	π_c, mN/m
SA	20	18	43
SA on AC protein subphase	90	18	43

Table 1
SURFACE CHARACTERISTICS OF SA MONOLAYER, IN THE ABSENCE AND THE PRESENCE OF AC PROTEIN. THE MEAN AREA VALUES, Å²/MOLECULE OF SA, FOR A_0 AND A_C AND COLLAPSE PRESSURE, π_c IN mN/m.

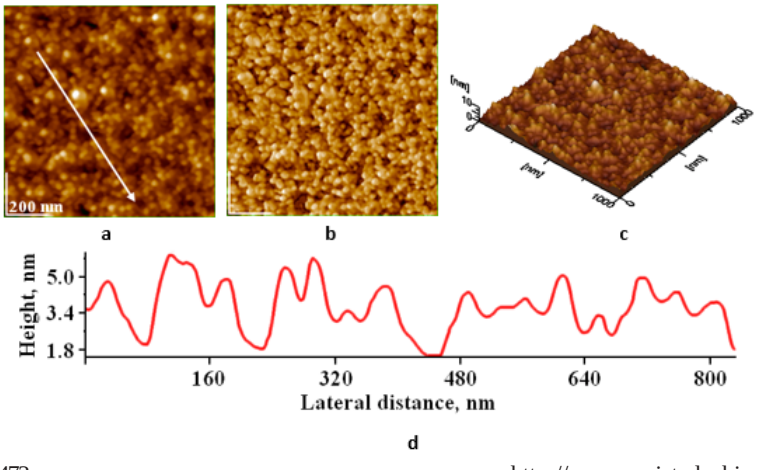

Fig. 2. AFM images of AC protein compact layer adsorbed on glass: 2D topography (a), phase image (b), 3D-topography (c) and cross profile (d) along the arrow given in panel (a). Scanned area 1 ìm x 1 ìm, RMS on area 1.18 nm

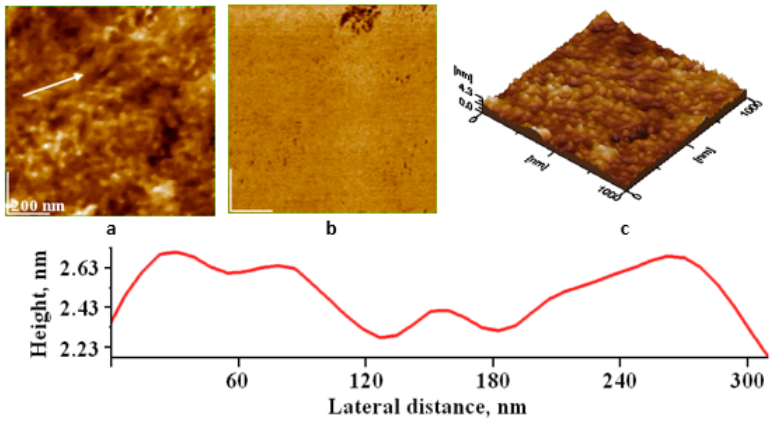

Fig. 3. AFM images of SA monolayer transferred on glass at 3 mN/m. Symbols as in figure 2. RMS on area 0.46 nm.

In the case of pure SA monolayer, for LB transferred at 3 mN/m from air/aqueous solution on glass support, the AFM images (figs. 3a-3c) revealed a rather porous SA nanostructure (fig. 3a) formed from large domains (e.g., hundreds of nm) with height of about 2.3 to 2.6 nm (fig. 3d), corresponding to well packed SA molecules. This SA structure is characteristic for SA condensed liquid monolayers [48]. The upper surface of pure SA monolayer is very flat, as it is given by RMS value of 0.46 nm.

AFM was also used coupled with LB technique to visualize the self-assemblies of mixed SA/AC protein layers transferred at various constant surface pressures, such as 3 mN/m (fig. 4), 20 mN/m (fig. 5) and 35 mN/m (fig. 6) from air/aqueous solutions to glass surface. The AFM images of mixed SA/AC protein self-assemblies clearly revealed their nano scale structure in substantial agreement with their molecular structure and with particle shape of AC protein.

AFM images indicate that the AC protein nanoparticles, formed by protein adsorption at the SA interfacial monolayer, are embedded into the SA porous network of the condensed liquid SA monolayer preferably at low surface pressure (e.g., 3 mN/m, fig. 4a-4c). Furthermore, the SA molecules simultaneously occupy the protein inter-particle spaces. It is also to be observed several aggregates or clusters of nanoparticles of AC protein, as brightest areas within the mixed SA/AC protein interfacial layer (fig. 4a). This morphology is in total agreement with the fact that the SA monolayer expands in the presence of adsorbed AC protein (fig. 1). From cross section profile (fig. 4d) the AC protein particles are shown and their diameter can be estimate, as about 55 nm.

In addition, SA molecules can also cover the outer surface of AC protein particles, which are attached directly beneath the carboxylic polar groups and carboxylate ions of SA monolayer, existing at the chosen *p*H of 5.3. Therefore, it is rational to propose that AC protein is bound to both negatively charged SA and to non-charged SA molecules, by electrostatic interactions and hydrogen bonds, within mixed interfacial layer. As expected, the RMS value is only slightly increased to 1.27 nm in comparison with RMS for pure SA monolayers.

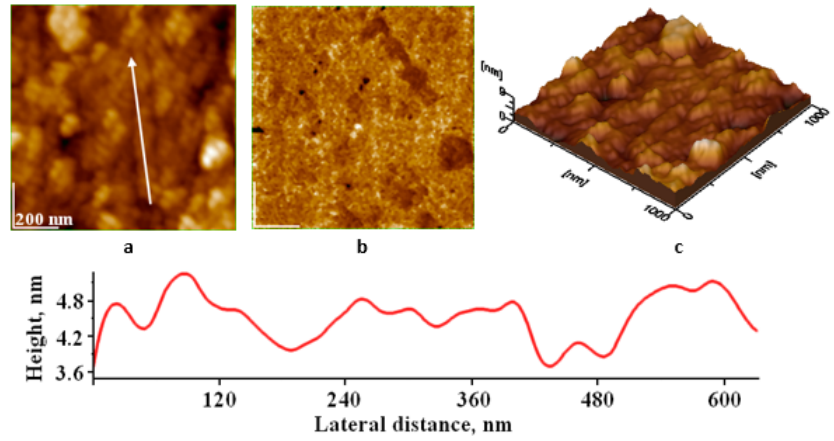

Fig. 4. AFM images of AC protein and SA self-assemblies transferred on glass at 3 mN/m. Symbols as in figure 2. RMS on area 1.27 nm.

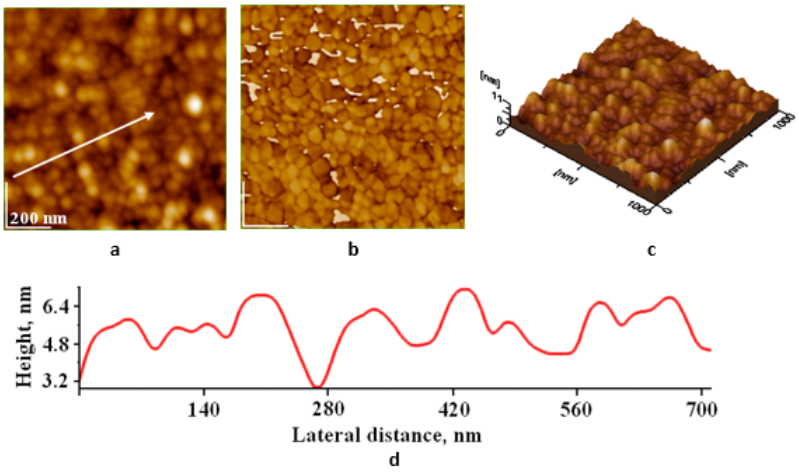

Fig. 5. AFM images of AC protein and SA self-assemblies transferred on glass at 20 mN/m. Symbols as in

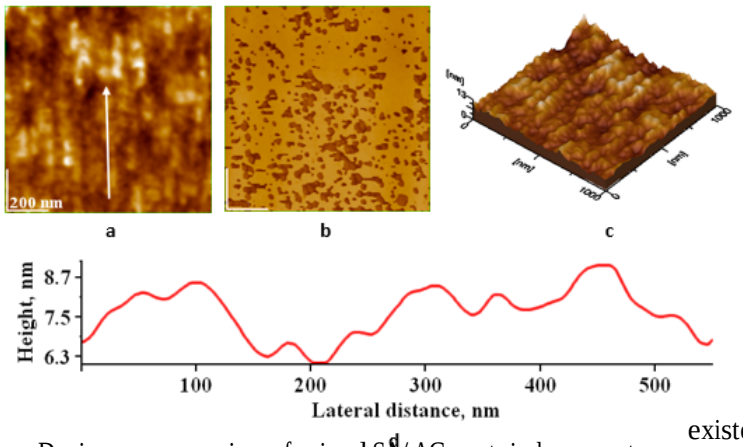

Fig. 6. AFM images of AC protein and SA self-assemblies transferred on glass at 35 mN/m. Symbols as in figure 2. RMS on area 1.33 nm.

During compression of mixed SA/ AC protein layers, at 20 mN/m, the resulting nanostructure (fig. 5a-5d) is formed primarily from AC protein nanoparticles, covered by SA molecules, and well packed within the mixed self-assemblies. Interestingly, the size of AC protein particles is almost constant (fig. 5d) of about 55 nm, as in figure 4d. This result shows that the AC protein nanoparticles covered by SA molecules are practically unmodified under these conditions. However, the height of the mixed layer is increased at 11 nm (fig. 5c), against its value of 9 nm, found at 3mN/m (fig. 4c). The RMS value is about 1.41 nm, and indicates again a low surface roughness for these mixed assemblies. A tendency of row formation can be also observed in figure 5a.

Compressing further the mixed SA/AC protein interfacial layer at 35 mN/m, corresponding to the solid state of pure SA monolayers (fig. 1), the AFM images (fig. 6a-6c) indicate a very well packed nanoparticles of AC protein covered by SA molecules, arranged in ordered lattice of almost parallel rows. The height of the mixed interfacial layer is increased to 13 nm (fig. 6c). The size of the AC nanoparticles covered by SA molecules obtained in cross profile (fig. 6d) is between 50 and 55 nm. The upper surface of mixed SA/AC protein layer is practically flat, and the RMS value of 1.33 nm is again rather low. This is also suitable for the deposition of an additional mixed layer, by high affinity of mixed SA/AC protein assemblies, thus opening the way for layer by layer building of multifunctional supramolecular assemblies.

The results obtained for mixed SA/AC protein layers revealed specific molecular interactions between these biologically relevant biocompounds, mainly due to AC protein adsorption on and its penetration into the SA monolayers leading to the mixed nanostructure formation in a similar way, as it was found with the interactions between cytochrome c and lipid structures [39].

The interplay between AC protein-AC protein molecular recognition and molecular self-organization of AC protein and SA molecules within the mixed interfacial layers leads to the complex multi-functional supramolecular nanostructures in which order and mobility are combined. Similar situation was also found with specific recognition and interaction between membrane-bound ligands and receptor proteins [38]. In these systems, the biological and biophysical function is based on the supramolecular organization.

Alternatively, the presence of SA monolayers may promote an enhanced adsorption of AC protein, leading to the formation of interfacial AC protein particles, which are embedded into the lipid matrix, and accordingly, the mixed interfacial supramolecular structures are developed. The AC protein particles are able to penetrate and especially expand the SA monolayers at low surface pressures and this effect might be explained at least in part due to the existence of high desorption energy of globular protein particles from interfacial layer [58].

Moreover, the nanoparticles of AC protein can stabilize the SA monolayer at the air/water interface by forming, through AC protein adsorption, a dense, close-packed layer at the SA monolayer surface that acts as a steric barrier against the SA monolayer collapse. A similar situation is reported for emulsions stabilized by silica particles [60], as a result of particle accumulation in a dense layer bridging the emulsion droplets.

Conclusions

We have used stearic acid, as a lipid model, and natural AC protein to develop supramolecular systems and to simulate the formation of storage lipid and protein assemblies within aleurone layers.

To our knowledge, this is the first demonstration of the formation of ordered mixed arrangements made of the AC protein and SA molecules within the interfacial layers, by using a combination of LB technique and AFM imaging. This approach has revealed to be appropriate and useful in the investigation of lipid and protein interactions. The obtained results pointed out that the AC protein is strongly attached to the stearic acid monolayers and the obtained interfacial arrangements are densely packed lipid-protein assemblies.

These results also revealed a high stability of the mixed interfacial layers, formed by ordered arrangements of lipid molecules and protein particles, which may contribute to the understanding of the formation of aleurone mixed lipid and protein granules, in vivo.

Undoubtedly, this biophysical chemistry approach might be widely used to investigate various biological assemblies made of lipids and globular proteins and can offer inspiring assessments in nanobiotechnology.

References

1. YUPSANIS, T., BURGESS, S.R., JACKSON, P.J., SHEWRY, P.R., J. Exp. Botany, **41,** 1990, p. 385.
2. SWANSON, S.J., BETHKE, P.C., JONES, R.L., The Plant Cell, **10,** 1998, p. 685.
3. HERMAN, E.M., LARKINS, B.A., The Plant Cell, **11,** 1999, p. 601.
4. RITCHIE, S., SWANSON, S.J., GILROY, S., Seed Sci. Research., **10,** 2000, p. 193.
5. SHEWRY, P.R., HALFORD, N.G., J. Exp. Botany, **53,** 2002, p. 947.
6. FATH, A., BETHKE, P., BELIGNI, V., JONES, R., J. Exp. Botany, **53**, nr. 372, 2002, p. 1273.
7. BOREN, M., LARSSON, H., FALK, A., JANSSON, C., Plant Sci., **166,** 2004, p. 617.
8. BECRAFT, P.W., YI, G., J. Exp. Botany, **62**, nr. 5, 2011, p. 1669.
9. ZHENG, Y., WANG, Z., Plant Cell Reports, **33**, nr. 10, 2014, p. 1607.
10. JONES, R.L., Plant Physiology, **44**, 1969, p. 1428.
11. JONES, R.L., Planta, **85**, 1969, p. 359.

12. TOMOAIA COTISEL, M., Multifunctional nanostructures formed of gold or silver nanoparticles and different biomolecules with medical applications, E-Book, Cluj University Press, Cluj-Napoca, 2016.
13. TOMOAIA-COTISEL, M., MOCANU, A., LEOPOLD, N., VASILESCU, M., CHIS, V., COZAR, O., J. Optoelectron. Adv. M., **9**, nr. 3, 2007, p. 637.
14. BRATU, I., TOMOAIA–COTISEL, M., DAMIAN, G., MOCANU, A., J. Optoelectron. Adv. M., **9**, nr. 3, 2007, p. 672.
15.TOMOAIA COTISEL, M., Convergence of Micro-NanoBiotechnologies, Series in Micro and Nanoengineering, Vol. 9, Editors: Zaharescu, M., Burzo, E., Dumitru, L., Kleps, I., Dascalu, D., Romanian Academy Press, Bucharest, 2006, p. 147.
16. TOMOAIA-COTISEL, M., TOMOAIA-COTISEL, A., YUPSANIS, T., TOMOAIA, G., BALEA, I., MOCANU, A., RACZ, C., Rev. Roum. Chim.(Bucharest), **51**, no. 12, 2006, p. 1181.
17) BANCIU, H., OLARU, F., HENGST, V., BANCIU, M., PETRESCU, I., MOCANU, A., TARBA, C., YUPSANIS, T., TOMOAIA-COTISEL, M., Studia, Univ. Babes-Bolyai, Biol., **52**, nr. 1, 2007, p. 37.
18) HOROVITZ, O., TOMOAIA, G., MOCANU, A., YUPSANIS, T., TOMOAIA-COTISEL, M., Gold Bulletin, **40**, nr. 3, 2007, p. 213.
19) HOROVITZ, O., TOMOAIA, G., MOCANU, A., YUPSANIS, T., TOMOAIA COTISEL, M., Gold Bulletin, **40**, nr. 4, 2007, p. 295.
20. TOMOAIA-COTISEL, M., HOROVITZ, O., BOROSTEAN, O., BOBOS, LD., TOMOAIA, G., MOCANU, A., YUPSANIS, T., Studia, Univ. Babes-Bolyai, Chem., **53**, nr. 1, 2008, p. 143.
21. TOMOAIA, G., HOROVITZ, O., MOCANU, A., NITA, A., AVRAM, A., RACZ, C.P., SORITAU, O., CENARIU, M., TOMOAIA-COTISEL, M., Colloids and Surfaces B: Biointerfaces, **135**, 2015, p. 726.
22. LOHCHAROENKAL, W., WANG, L., CHEN, Y.C., ROJANASAKUL, Y., BioMed. Research International, **2014**, 2014, Article ID 180549, 12 pages; http://dx.doi.org/10.1155/2014/180549
23. DUCEL, V., RICHARD, J., POPINEAU, Y., BOURY, F., Biomacromolecules, **5,** 2004, p. 2088.
24. TOMOAIA, G., TOMOAIA-COTISEL, A., TOMOAIA-COTISEL, M., MOCANU, A., Open Chemistry, **3**, nr. 2, 2005, p. 347.
25. JOOS, P., TOMOAIA-COTISEL, A., SELLERS, A.J., TOMOAIA-COTISEL, M., Colloids and Surfaces B: Biointerfaces, **37**, nr. 3, 2004, p. 83.
26. ZSAKO, J., TOMOAIA-COTISEL, M., CHIFU, E., MOCANU, A., FRANGOPOL, P.T., Biochim. Biophys. Acta, **1024**, nr. 2, 1990, p. 227.
27. ZSAKO, J., TOMOAIA-COTISEL, M., CHIFU, E., J. Colloid Interface Sci., **102**, nr. 1, 1984, p. 186.
28. TOMOAIA-COTISEL, M., ZSAKO, J., MOCANU, A., LUPEA, M., CHIFU, E., J. Colloid Interface Sci., **117**, nr. 2, 1987, p. 464.
29. TOMOAIA COTISEL, M., ZSAKO, J., CHIFU, E., QUINN, P.J., Chem. Phys. Lipids, **34**, nr. 1, 1983, p. 55.
30. ZSAKO, J., TOMOAIA-COTISEL, M., CHIFU, E., J. Colloid Interface Sci., **146**, nr. 2, 1991, p. 353.
31. TOMOAIA COTISEL, M., CHIFU, E., ZSAKO, J., MOCANU, A., QUINN, P.J., KATES, M., Chem. Phys. Lipids, **63**, nr. 1-2, 1992, p. 131.
32. TOMOAIA COTISEL, M., ZSAKO, J., CHIFU, E., Ann. Chim. (Rome), **71**, nr. 3-4, 1981, p. 189.
33. TOMOAIA-COTISEL, M., SEN, A., QUINN, P.J., J. Colloid Interface Sci., **94**, nr. 2, 1983, p. 390.
34. TOMOAIA COTISEL, M., Progr. Colloid Polym. Sci., **83**, 1990, p. 155.
35. TOMOAIA COTISEL, M., CADENHEAD, D.A., Langmuir, **7**, 1991, p. 964.
36. ASGHARIAN, B., CADENHEAD, D.A., TOMOAIA-COTISEL, M., Langmuir, **9**, 1993, p. 228.
37. VERGER, R., PATTUS, F., Chem. Phys. Lipids, **30**, nr. 2-3, 1982, p. 189.
38. AHLERS, M., MULLER, W., REICHERT, A., RINGSDORF, H., Angewandte Chimie, **29,** nr. 11, 1990, p. 1269.
39. KOZARAC, Z., DHATHATHREYAN, A., MOBIUS, D., FEBS Letters, **229,** nr. 2, 1988, p. 372.
40. BROCKMAN, H., Current Opinion in Structural Biology, **9**, nr. 4, 1999, p. 438.
41. REVIAKINE, I., BERGSMA-SCHUTTER, W., BRISSON, A., Journal of Structural Biology, **121**, 1998, p. 356.
42. DHAR, P., ECK, E., ISRAELACHVILI, J.N., LEE, D.W., MIN, Y., RAMACHANDRAN, A., WARING, A.J., ZASADZINSKI, J.A., Biophysical J., **102**, 2012, p. 56.
43. BORRELL, J.H., MONTERO, M.T., MORROS, A., DOMENECH, O., J. Mol. Recognit., **28,** nr. 11, 2015, p. 679.
44. MASHAGHI, S., JADIDI, T., KOENDERINK, G., MASHAGHI, A., Int. J. Mol. Sci., **14**, 2013, p. 4242.
45. TOMOAIA COTISEL, M., MOCANU, A., Rev. Chim. (Bucharest), **59**, 2008, p. 1230.
46. FRANGOPOL, P.T., CADENHEAD, D.A., TOMOAIA-COTISEL, M., MOCANU, A., Studia, Univ. Babes-Bolyai, Chem., **54**, nr. 1, 2009. p. 23.
47. FRANGOPOL, P.T., CADENHEAD, D.A., TOMOAIA, G., MOCANU, A., TOMOAIA-COTISEL, M., Rev. Roum. Chim., **60**, nr. 2-3, 2015, p. 265.
48. TOMOAIA-COTISEL, M., TOMOAIA, G., POP, V.D., MOCANU, A., APETROAEI, N., POPA, G., Rev. Roum. Chim., **50**, nr. 5, 2005, p. 381.
49. TOMOAIA, G., SORITAU, O., TOMOAIA-COTISEL, M., POP, L.B., POP, A., MOCANU, A., HOROVITZ, O., BOBOS, L.D., Powder technology, **238**, 2013, p. 99.
50. TOMOAIA, G., POP, L.B., PETEAN, I., TOMOAIA-COTISEL, M., Mater. Plast., **49**, nr. 1, 2012, p. 48.
51. TOMOAIA, G., MOCANU, A., VIDA-SIMITI, I., JUMATE, N., BOBOS, L.D., SORITAU, O., TOMOAIA-COTISEL, M., Materials Science and Engineering: C-Materials for Biological Applications, **37**, 2014, p. 37.
52. ZDRENGHEA, U.V., TOMOAIA, G., POP-TOADER, D.V., MOCANU, A., HOROVITZ, O., TOMOAIA-COTISEL, M., Combinatorial chemistry & high throughput screening, **14**, nr. 4, 2011, p. 237.
53. BARBU TUDORAN, L., TOMOAIA, G., HOROVITZ, O., MOCANU, A., TOMOAIA COTISEL, M., J. Optoelectron. Adv. M., **10**, nr. 9, 2008, p. 2293.
54. MOCANU, A., PASCA, R.D., TOMOAIA, G., GARBO, C., FRANGOPOL, P.T., HOROVITZ, O., TOMOAIA COTISEL, M., Int. J. Nanomed., **8,** 2013, p. 3867.
55. NAGHIU, M.A., GOREA, M., MUTCH, E., KRISTALY, F., TOMOAIA-COTISEL, M., Journal of Materials Science & Technology, **29**, nr. 7, 2013, p. 628.
56. FURTOS, G., NAGHIU, M.A., DECLERCQ, H., GOREA, M., PREJMEREAN, C., PANA, O., TOMOAIA COTISEL, M., Journal of Biomedical Materials Research, Part B: Applied Biomaterials, **104**, nr. 7, 2016, p. 1290.
57. TCHOLAKOVA, S., DENKOV, N.D., LIPS, A., **Phys. Chem. Chem. Phys., 10**, nr. 12, 2008, p. 1608.
58. AMIN, S., BARNETT, G.V., PATHAK, J.A., ROBERTS, C.J., SARANGAPANI, P.S., Current Opinion in Colloid Interface Sci., **19**, 2014, p. 438.
59. DAS, T.K., AAPS Pharm. Sci. Tech., **13**, nr. 2, 2012, p. 732.
60. HOROZOV, T.S., BINKS, B.P., Angewandte Chemie, **45**, nr. 5, 2006, p. 773.

Manuscript received: